Extended Abstracts of the 2006 International Conference on Solid State Devices and Materials, Yokohama, 2006, pp. 634-635

P-7-1

Lock-in pixel using a Current-assisted photonic demodulator Implemented in 0.6µm Standard CMOS

Ward van der Tempel, Daniël Van Nieuwenhove, Riemer Grootjans and Maarten Kuijk

Vrije Universiteit Brussel, Laboratory for Micro- & Photonelectronics (LAMI),
Pleinlaan 2, 1050 Brussels, Belgium
Email : (wvdtemp, davnieuw, rgrootja, mkuijk) @etro.vub.ac.be

1. Introduction

Artificial three-dimensional vision systems are a thing long since dreamed of. It is the missing link between a lot of intelligent systems and the outside world, enabling machines to actually perceive the world as we see it, in 3D.

The Time-of-Flight principle provides an elegant solution to this problem. Recently a lot of effort has been put in the creation of photonic demodulators [1],[2],[3]. These structures enable 3D imaging systems using the Time-of-Flight principle. In this paper we will highlight the assets of the photonic demodulation structure we propose, and report a lock-in pixel based on this detector.

2. The principle of operation of a current assisted photonic demodulator

The operation principle of this photonic demodulator was proposed in [4]. A majority current through the substrate is used to guide the electrons generated by light impinging on the substrate towards a detecting junction. By alternating the direction of the majority carrier current, the electrons can be transferred towards distinct detection junctions. In this way, modulated incident light can be demodulated.

Figure 1 shows a cross-section of the detector. A majority current is sustained in the substrate by a potential ΔV applied between substrate contacts Mix2 and Mix1, with $V_{mix2}>V_{mix1}$ (ΔV>0). The electrons generated by light impinging on the substrate are transferred to the detecting junction. The transfer mechanism is drift, provided by the electric field induced in the substrate. By applying a negative ΔV, the direction of the current is inverted, as well as the electric field induced in the substrate. The electrons are transferred away from the detecting junction, virtually switching the detector OFF.

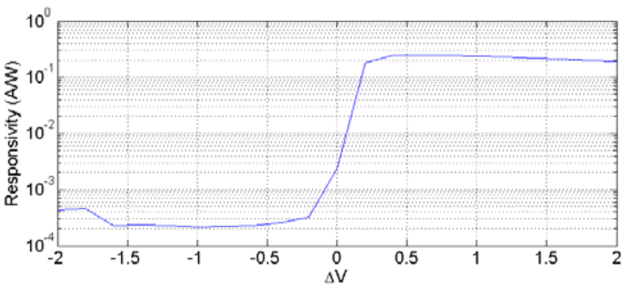

Figure 2 - Static behaviour of the detector. Responsivity of up to 0.26A/W is obtained when applying a positive ΔV. The detector is virtually switched OFF with a negative ΔV.

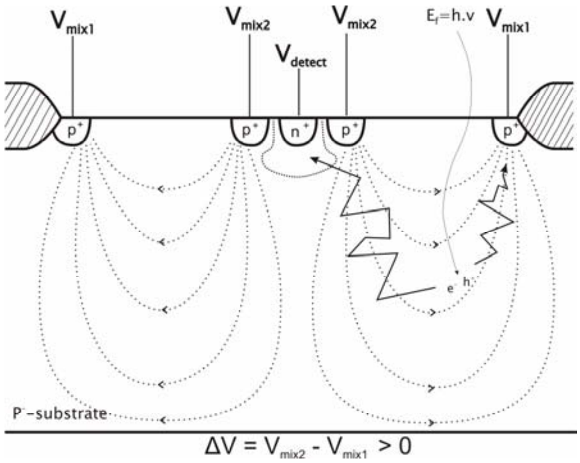

Figure 1 - A potential ΔV>0 is applied, creating an electric field in the substrate. The electrons are transferred through drift to the detection junction. By applying ΔV<0, the electrons are transferred away from the detection junction.

A detector, measuring 30umx30um, is implemented according to this scheme in 0.6micron Standard CMOS technology. Figure 2 shows the efficiency in A/W of the detector as a function of ΔV. We obtained a maximum responsivity of 0.26 A/W with a ΔV of only 0.8V and λ=860nm infra-red light. We also obtained a static demodulation contrast of close to 100%.

3. Lock-in pixel – Architecture and operation

Using this current assisted demodulator, a lock-in pixel was designed. The goal of this pixel is to be able to measure the phase-shift of a detected modulated optical signal with respect to the original modulation signal. The structure of the pixel is shown in Figure 3. The pixel architecture is analogous to CMOS Active Pixels. It consists of the current assisted photonic demodulator, operated with the 2 modulation signals Mix1 and Mix2, which are in counter-phase. It also consists of a 360 fF poly1-poly2-capacitor Cap1, a reset-transistor M1 and a source-follower M2 – M3. The incident optical signal is demodulated, and the resulting charges are detected with D1 and integrated on the capacitance of node 1.

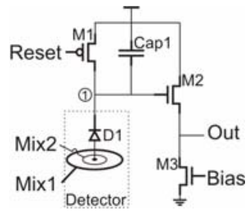

Figure 3 - Pixel architecture

The operation of the pixel is analogous to a CMOS Active Pixel. The detected charges are integrated over a set integration time t_{int}, the voltage on node 1 is read out through the source-follower, and then reset through M1. In this pixel however, before detection in D1, the photo-generated signal is mixed with the signal applied on Mix1/Mix2 (Mix2 is in counter-phase with Mix1).

Suppose both the device and the optical signal are modulated with a sine wave with a certain frequency f_1, amplitude normalized to 1, and a phase offset equal to zero. This signal is represented by a vector S_0 in the polar plot relative to f_1 in Figure 4. The optical signal is sent along a path of unknown length. It experiences a phase-shift φ, and is captured by the detector. The resulting signal can be represented by the vector R. The lock-in pixel mixes the signal sent to the device with the captured signal. Mixing R with the original signal S_0 yields the projection I. In order to reconstruct φ, a second projection Q is needed by mixing R with the vector S_{90} which is S_1 with an offset of 90°. In this way, the photonic demodulator can deduct the traveling time of the optical signal by measuring the phase-shift φ.

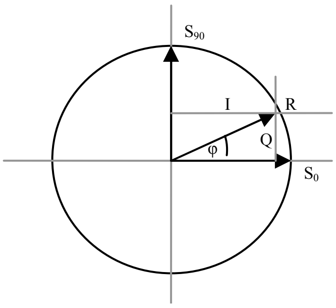

Figure 4 - Polar plot of modulation signals S and Detected optical signal R.

In practice, 2 more correlations need to be measured to eliminate errors caused by background illumination and the amplitude of the optical signal. Additionally, the pixel will only extract phase information of incident optical signals with frequency f_1, since inter-frequency correlations are 0. Hence this pixel is called a lock-in pixel.

4. Phase measurements

The phase measurements with the pixel were performed with a setup that artificially applies a phase-shift of the optical signal, simulating the shift due to traveling time. The pixel receives this optical signal and measures the correlations discussed above. An infra-red laser with λ=860nm was used in all measurements. The mixing potential ΔV was switched between 1V and -1V to create the alternating drift field in the substrate. Square waves were used as modulating signal. We obtained a demodulation contrast of above 90% up to a demodulation frequency of 2MHz, using λ=860nm light. Compared to previous work on CMOS PMD devices, done by R. Lange et al. [2] this is a serious improvement (Figure 5). This demodulation bandwidth of 2MHz is lower than in [4] because of the use of a different technology and the application of a weaker drift field.

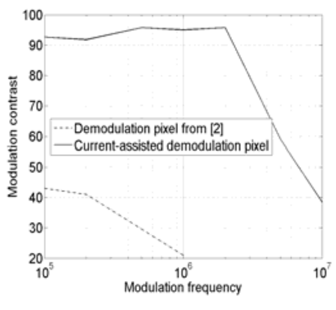

Figure 5 - Comparison of demodulation contrast of the Standard CMOS PMD from [2] and of the current-assisted photonic demodulator

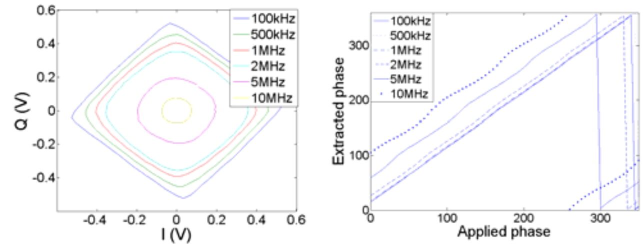

Figure 6 - Left : Measured I,Q-plot. Right : Extracted phase calculated with the measured correlation values versus the artificially applied phase of the optical signal.

Figure 6 - Left shows the I-Q-plot we obtained at various frequencies. When using square waves, this I-Q plot should have a diamond shape, which is the case up to the demodulation bandwidth. Beyond that frequency, the IQ-plot converges to a circle. This is as if the modulation signal would have been a sine wave. Figure 6 – Right shows the phase shift calculated using the measured correlations I and Q, as a function of the artificially applied phase of the sent optical signal. These calculations were based on the square wave approximation, using equations valid for an ideal diamond shape IQ plot. It shows that the pixel has a linear phase response up to 2 MHz. Using adequate calculations based on sine wave equations, a linear phase graph can be obtained beyond the demodulation bandwidth at frequencies up to 10MHz.

5. Conclusions

We showed a Standard CMOS compatible photonic mixer implemented in 0.6um technology with a responsivity of 0.26A/W. We also obtained a nearly 100% demodulation contrast at DC, a demodulation contrast above 90% up to 2MHz with λ=860nm infra-red light. Furthermore we reported a lock-in pixel based on this detector, with a linear phase graph up to 2MHz, and even beyond the demodulation bandwidth up to 10MHz with the appropriate calculations.

6. References

[1] Schwarte, R., *Dynamic 3D-Vision,* 2001 International Symposium on Electron Devices for Microwave and Optoelectronic Applications, 15-16 Nov. 2001 Page(s):241 – 248.

[2] Lange, R. and Seitz, P., *Solid-state time-of-flight range camera,* IEEE Journal of Quantum Electronics, Volume 37, Issue 3, March 2001 Page(s):390 – 397.

[3] Izhal, A.H.; Ushinaga, T.; Sawada, T.; Homma, M.; Maeda, Y.; Kawahito, S., *A CMOS Time-of-Flight Range Image Sensor with Gates on Field Oxide Structure*, Sensors, 2005 IEEE, Oct. 31, 2005 Page(s): 141 – 144.

[4] Van Nieuwenhove, D.; van der Tempel, W.; Kuijk, M, *A Novel Standard CMOS Detector using Majority Current for guiding Photo-Generated Electrons towards Detecing Junctions*, Proceedings Symposium IEEE/LEOS Benelux Chapter, 2005, Pages: 229 – 232.